

J.F. Justin, A. Jankowiak  
(Onera)

E-mail: jean-francois.justin@onera.fr

## Ultra High Temperature Ceramics: Densification, Properties and Thermal Stability

Hypersonic flights, re-entry vehicles, and propulsion applications all require new materials that can perform in oxidizing or corrosive atmospheres at temperatures in excess of 2000°C and sometimes over the course of a long working life. Ultra High Temperature Ceramics (UHTCs) are good candidates to fulfill these requirements. Within this family, the ZrB<sub>2</sub> and HfB<sub>2</sub> based composites are the most attractive. The oxidation resistance of diboride-based compounds is better than that of SiC-based ceramics thanks to the formation of multi-oxide scales composed of a refractory oxide (skeleton) and a glass component. Onera is actively involved in several programs to develop such materials for both hypersonic civilian flights and for propulsion systems.

In this paper, we present the ZrB<sub>2</sub>-SiC, ZrB<sub>2</sub>-SiC-TaSi<sub>2</sub> and HfB<sub>2</sub>-SiC-TaSi<sub>2</sub> composites developed in the Onera laboratories for leading edges or air intakes of future hypersonic civilian aircrafts flying up to Mach 6 (T~1100°C-1500°C) with comparisons with the state of the art. Then we discuss new perspectives for higher temperature applications (T>2000°C).

### Introduction

Ultra High Temperature Ceramics (UHTCs) are good choices for several extreme applications: thermal protection materials on hypersonic aerospace vehicles or re-usable atmospheric re-entry vehicles, specific components for propulsion, furnace elements, refractory crucibles, etc. This family of ceramic compounds is made of borides, carbides and nitrides such as ZrB<sub>2</sub>, HfB<sub>2</sub>, ZrC, HfC, TaC, HfN which are characterized by high melting points (table 1), high hardness, chemical inertness and relatively good resistance to oxidation in severe environments.

Historically, this family of ceramic materials was first investigated between the 1950s and 1970s by Russian and U.S. laboratories [1][2], but recent studies to develop hypersonic flight vehicles in particular have led to a resurgence of interest. For hypersonic vehicles with sharp aerosurfaces (engine cowl inlets, wing leading edges and nosecones), there are foreseeable needs for materials that can withstand temperatures of 2000 to 2400°C, operate in air and be re-usable [3]. At present, the structural materials for use in high-temperature oxidizing environments are limited to SiC and Si<sub>3</sub>N<sub>4</sub> based materials, oxide ceramics and C/C composites with thermal protection. Silicon-based ceramics and protected C/C composites exhibit good oxidation resistance, but only up to ~1600°C, and their thermal

cycling lifetimes are modest. The development of structural materials for use in oxidizing and rapid heating environments at temperatures above 1600°C is therefore of great importance for engineering.

Material	Crystal structure	Density (g/cm <sup>3</sup> )	Melting température (°C)
HfB <sub>2</sub>	Hexagonal	11.2	3380
HfC	Face-centered cubic	12.76	3900
HfN	Face-centered cubic	13.9	3385
ZrB <sub>2</sub>	Hexagonal	6.1	3245
ZrC	Face-centered cubic	6.56	3400
ZrN	Face-centered cubic	7.29	2950
TiB <sub>2</sub>	Hexagonal	4.52	3225
TiC	Cubic	4.94	3100
TiN	Face-centered cubic	5.39	2950
TaB <sub>2</sub>	Hexagonal	12.54	3040
TaC	Cubic	14.50	3800
TaN	Cubic	14.30	2700
SiC	Polymorph	3.21	Dissociates 2545

Table 1 – Properties of some UHTCs

Since the 1950s, studies have revealed that diborides of the group IVB were the most resistant to oxidation and among these compounds,  $\text{HfB}_2$  was the best, followed by  $\text{ZrB}_2$ . However, the use of single-phase materials was not sufficient for high-temperature structural applications. Thus, many additives such as Nb, V, C, disilicides and SiC were evaluated to improve the resistance to oxidation. Of these additives, SiC seemed to be particularly valuable and 20 vol% was judged optimal for hypersonic vehicles by the US Air Force. At present, many groups in the U.S., Japan, China, India and in Europe (especially in Italy) are studying UHTC systems to improve resistance to oxidation [4][5][6][7]. Moreover, in comparison with carbides and nitrides, the diborides have also higher thermal conductivity, which gives them good thermal shock resistance and makes them ideal for many high-temperature thermal applications. For a leading edge for example, a high thermal conductivity reduces thermal stress within the material by lowering the magnitude of the thermal gradient inside the part. Furthermore, it allows energy to be conducted away from the tip of the piece and re-radiated out of the surfaces of the component with lower heat fluxes [8]. Diboride-based UHTCs also exhibit high electrical conductivity (table 2), which is appreciable for manufacturing complex shape components for example (by using Electrical Discharge Machining).

Over the past five years, Onera has carried out several activities on UHTC materials. This paper is an outline of the work which has been done on these materials in the Composite Materials and Structures Department. First, we describe the  $\text{ZrB}_2$ -SiC,  $\text{ZrB}_2$ -SiC-TaSi<sub>2</sub> and  $\text{HfB}_2$ -SiC-TaSi<sub>2</sub> composites developed for leading edges or air intakes of the ATLLAS vehicle (future hypersonic civil aircraft flying up to Mach 6) in comparison with the state of the art. In conclusion, new perspectives and compositions for higher temperature applications ( $T > 2000^\circ\text{C}$ ) are discussed.

Property	$\text{ZrB}_2$	$\text{HfB}_2$
Crystal system space group prototype structure	Hexagonal $P6/mmm A1B_2$	Hexagonal $P6/mmm A1B_2$
a (Å)	3.17	3.139
c (Å)	3.53	3.473
Density (g/cm <sup>3</sup> )	6.1	11.2
Melting temperature (°C)	3245	3380
Young's modulus (GPa)	489	480
Hardness (GPa)	23	28
Coefficient of Thermal Expansion (°C <sup>-1</sup> )	$5.9 \times 10^{-6}$	$6.3 \times 10^{-6}$
Heat capacity at 25°C (J.mol <sup>-1</sup> .°C <sup>-1</sup> )	48.2	49.5
Thermal conductivity (W.m <sup>-1</sup> .°C <sup>-1</sup> )	60	104
Electrical conductivity (S/m)	$1.0 \times 10^7$	$9.1 \times 10^6$

Table 2 – Summary of some properties of  $\text{ZrB}_2$  and  $\text{HfB}_2$  [9]

## Future hypersonic aircraft materials

### Context

In 2006, the European Community launched a 3-year project called ATLLAS (Aerodynamic and Thermal Load Interactions with Lightweight Advanced Materials for High Speed Flight) to initiate research on high-

temperature resistant materials for sustained hypersonic flight (up to Mach 6). The project [10], led by ESA-ESTEC, consists of a consortium of 13 partners from industry, research institutions and universities (ASTRIUM, EADS-IW, MBDA, ALTA, GDL, DLR, FOI, ONERA, SOTON, ITR, TUM, UPMC and ESA-ESTEC). Within this program, ONERA DMSC has the objective of investigating and manufacturing materials to allow for the designing of sharp leading edges or air intakes for the ATLLAS reference vehicle [11]. For hypersonic vehicles, performance improvement (lift-to-drag ratio in particular) requires slender aerodynamic shapes with sharp leading edges. However, the thinner the leading edge radius, the higher the temperature. Successful designs for hypersonic aircraft therefore require the development of new materials with higher temperature capabilities.

The first part of the study focused on the choice of suitable compositions to define UHTC solutions for slender aerodynamic shapes. The selection was based on four different criteria: the requirements for these applications (see box 1) taking into account the flight parameters of the ATLLAS vehicle (speed, altitude, etc.) and the shape of the piece (sweep back angle, tip radius, etc.), the processing methods available at Onera, the bibliographical results on similar applications and the thermodynamic stability predictions of the selected compositions. According to these criteria, a preliminary selection of three compositions that are feasible by hot pressing [12] [13] (expected sintering temperature between 1600 and 2000°C), has been done:

- $\text{ZrB}_2$  (60 vol%) + SiC (20 vol%) + TaSi<sub>2</sub> (20 vol%)
- $\text{HfB}_2$  (60 vol%) + SiC (20 vol%) + TaSi<sub>2</sub> (20 vol%)
- $\text{ZrB}_2$  (80 vol%) + SiC (20 vol%)

In these compositions, silicon carbide additives are used firstly to enhance resistance to oxidation, secondly to promote densification by restricting the growth of diboride grains, and lastly to lower their sintering temperature [14]. According to several studies, additions of 20 vol% were judged optimal for our application. For tantalum disilicide additives, the objectives are to increase oxidation resistance and to reduce the sintering temperature of the powder blends [14][15] (the melting temperature of the TaSi<sub>2</sub> is “only” 2400°C). The addition of Ta to the system reduces the concentration of oxygen vacancies and decreases oxygen transport through the growing oxide scale and thus lowers the oxidation rate. Furthermore, Ta additions increase the oxide scale adhesion by phase stabilization. As for the last composition, it is a “classical”  $\text{ZrB}_2$ /SiC material. It has been studied in order to provide reference points for comparison with the first two compositions and the results from the literature.

### Experimental procedure

To obtain the three selected compositions, commercially available  $\text{ZrB}_2$ ,  $\text{HfB}_2$ , SiC and TaSi<sub>2</sub> powders (table 3) were used as precursors. The preparation of the blends involved three successive stages. First, to reduce particle size distribution and promote intimate mixing, the mixtures were ball milled in cyclohexane for several hours using Si<sub>3</sub>N<sub>4</sub> milling media in a high-density polyethylene tank. Rotary evaporation was then used to extract the solvent and minimize segregation during drying. Lastly, the powder blends were sieved to avoid agglomeration. During the study, various improvements were made to this cycle in order to obtain the purest mixtures: a significant decrease of the total duration of attrition, the use of YTZ (ZrO<sub>2</sub>) grinding media and optimization of the order of introduction of the constituents.

## Box 1 - Some requirements for UHTC materials in ATLLAS application

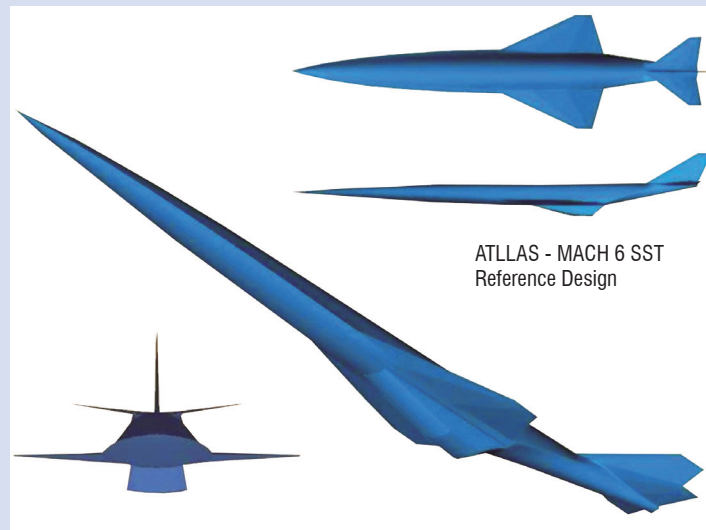
### ATLLAS objectives

Future hypersonic civil aircraft for flights at Mach 3 or Mach 6 with a cruising altitude of 30500 m. A minimum of 60 flights should be carried out at maximum speed. With these flight conditions, leading edge (L.E.) and nose temperatures between 980 and 1150°C are expected. The high temperature materials must have a service life of about 40,000 hours with more than 20,000 hours of exposure to the maximum thermal loads.

#### Details of the ATLLAS vehicle, the flight parameters and the shape of the wing

- Length = 105.1 m
- Wingspan = 29.7 m
- Gross Takeoff Weight = 278 tons (including 110 tons of hydrogen fuel)
- Number of passengers = 200
- Maximum speed = Mach 6
- Cruise altitude = 30 km
- Range = 9300 km (in fact only 7400 km)
- Service life > 25,000 cycles (~ 40,000 h)
- Angle of attack of the vehicle = 4°
- Wing L.E. sweep back angle = 65°
- Radius of curvature at the tip = 1 mm
- Maximum expected temperature = 1150°C (with an emissivity of 0.85)

#### Design of the reference vehicle



Designing UHTC components for hypersonic applications requires precise knowledge of the values of specific physical, thermal, mechanical and surface properties (density, coefficient of thermal expansion, specific heat, thermal conductivity, Young's modulus, Poisson's ratio, emissivity, catalytic efficiency, surface roughness, etc.) [16].

Starting powder	Particle size ( $\mu\text{m}$ )	Grade / supplier	Purity (%)
ZrB <sub>2</sub>	8.17	Z-1031 / Cerac	99.5
HfB <sub>2</sub>	1.99	H-1002 / Cerac	99.5
SiC	0.60	BF12 / H.C. Starck	>98.5
TaSi <sub>2</sub>	6.54	T-1016 / Cerac	99.5

Table 3 – Size, grade and purity of starting powders

The second phase of the process involved sintering the previous powder blends by hot pressing. This standard processing method has been successfully used to manufacture monolithic plates. The making of UHTCs often requires higher cost processes with high temperatures and pressures to obtain complete densification. In our sintering process, a resistance heated furnace using graphite dies was used. After the improvements in the mixture preparation, the selected densification parameters were finally the following:

- Sintering temperature 1700 T 1800°C
- Dwell time t = 2 hours
- Uniaxial pressure P = 27 MPa
- Atmosphere argon at atmospheric pressure after a first step under vacuum
- Graphite dies 36 x 36 mm<sup>2</sup>, 45 x 45 mm<sup>2</sup> and 68 x 68 mm<sup>2</sup>

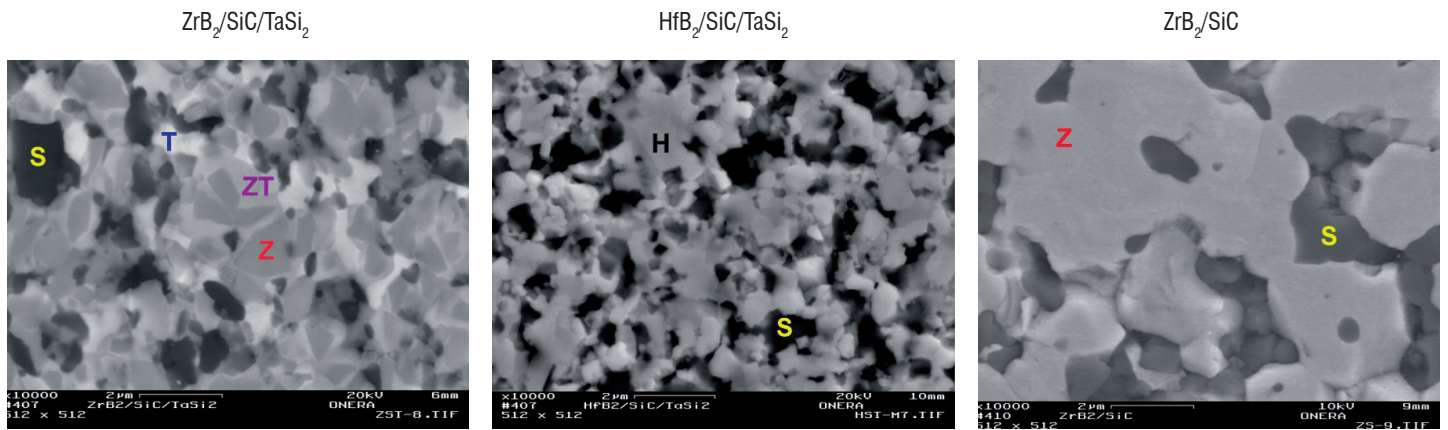
High densification rates are obtained on monoliths. The density of each material has been assessed by Archimedes' method. For the three sintered compositions, the open porosities are lower than 1 % and their densification rates are approximately 98 % of the theoretical value (table 4).

Composition	Apparent density/g/cm <sup>3</sup>	Open porosity
ZrB <sub>2</sub> /SiC	5.36±0.04	0.60±0.33
ZrB <sub>2</sub> /SiC/TaSi <sub>2</sub>	5.95±0.01	0.30±0.10
HfB <sub>2</sub> /SiC/TaSi <sub>2</sub>	9.09±0.13	0.38±0.21

Table 4 – Densification level

Furthermore, a very fine microstructure is obtained with good homogeneity and a small grain size (figure 1). In addition, despite the presence of high density compounds ( $\rho_{\text{HfB}_2} = 11.2 \text{ g/cm}^3$  and  $\rho_{\text{TaSi}_2} = 9.1 \text{ g/cm}^3$ ), the densest material (HfB<sub>2</sub>/SiC/TaSi<sub>2</sub>) exhibits a value that is not very far from that of some well-known metal alloys (Inconel 617 for instance,  $\rho = 8.4 \text{ g/cm}^3$ ).

Some X-Ray diffraction analyses were used to identify phases present in these materials. The results indicated the presence of the main constituents as foreseen but also some traces of Ta<sub>5</sub>Si<sub>3</sub>, ZrO<sub>2</sub>, HfO<sub>2</sub> and SiO<sub>2</sub>.



Material labels: Z for ZrB<sub>2</sub>, H for HfB<sub>2</sub>, S for SiC, T for TaSi<sub>2</sub> and ZT for (Zr,Ta)B<sub>2</sub>.

Figure 1 – Microstructure of each type of hot pressed material (SEM observations)

### Material properties

In order to estimate the capability of the previous monoliths to fulfill the requirements of hypersonic applications, several aspects have been investigated and in particular: machinability, physical, thermal and mechanical properties, resistance to oxidation, thermal shock behavior and resistance under high-enthalpy hypersonic flow (arc jet tests).

### Machinability

Materials based on hard and brittle constituents (borides, carbides and silicides) often involve expensive and difficult machining. In our case, thanks to the low electrical resistivity of the compounds which are present in our compositions, the use of Electrical Discharge Machining is perfectly possible ( $\rho_{ZrB_2} = 6$  to  $10 \mu\Omega \cdot \text{cm}$ ,  $\rho_{HfB_2} = 10$  to  $16 \mu\Omega \cdot \text{cm}$ ,  $\rho_{SiC} \sim 105 \mu\Omega \cdot \text{cm}$  and  $\rho_{TaSi_2} = 8$  to  $46 \mu\Omega \cdot \text{cm}$  [17]). All the selected materials can be easily machined by EDM, and the surfaces are clean and even (figure 2). This is one of the important advantages of these materials. It is important to note that, with EDM, complex shapes can also be made using a die-sinking machine, also known as a ram-type, plunge, or vertical erosion machine [18].

Furthermore, in this work, we have also demonstrated the good behavior of the selected materials for machining with the standard techniques (surface grinding with diamond tools for instance). Several samples

and prototypes were manufactured with this method. In particular, a small piece representing an air intake was made by diamond machining (figure 2). The objective was to test the feasibility of a prototype with a very thin tip. As expected, a small radius was obtained. In fact, the radius was well under the required value for the component (length = 40 mm, width = 40 mm, thickness = 1.9 mm and radius  $\sim 0.15$  mm). Thus, it is clearly possible to obtain very sharp pieces and acute angles.

### Mechanical performance

#### Elastic constants

Nine to twelve samples of each composition were tested with a Grindosonic MK5 apparatus to determine the elastic constants of these materials by impulse excitation of vibration [19]. In fact, due to the dimension of the available samples (bars of  $\sim 35.40 \times 5.20 \times 1.75 \text{ mm}^3$ ), it was only possible to measure the flexural resonant frequencies. Therefore, we were only able to determine the Young's modulus (table 5). The observed values are in good agreement with the expected results [20][21][22].

As for the other elastic constants, we note than similar materials have already been presented in the literature and they generally exhibit shear moduli close to 200 GPa and Poisson's ratios around 0.12 - 0.14 [20] [23].

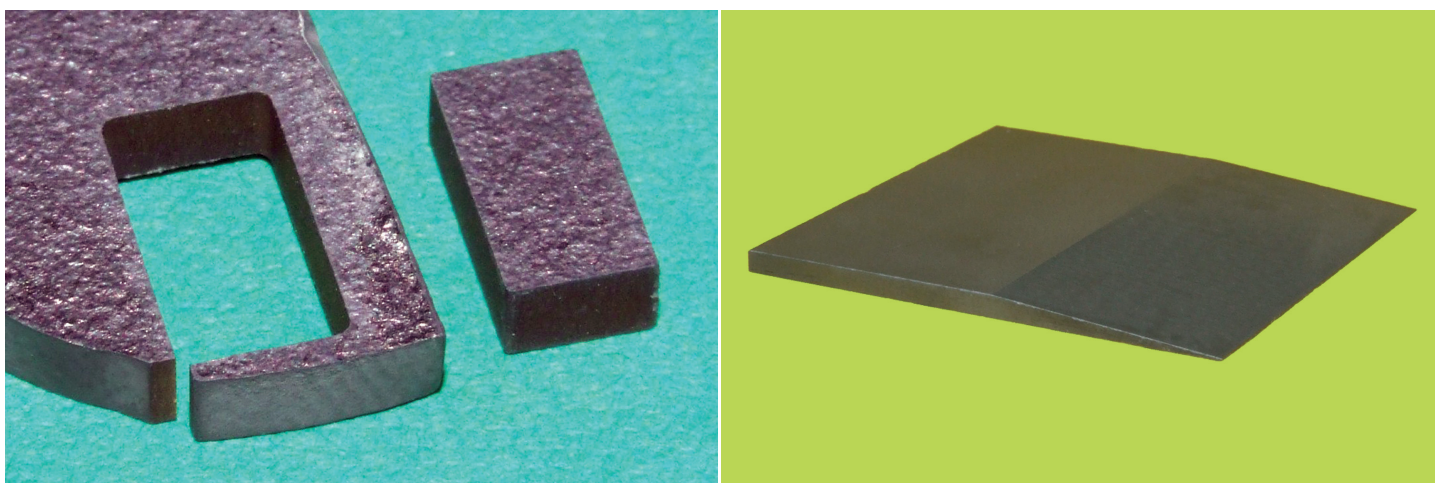


Figure 2 – Wire-cutting EDM trial (left) and a thin air intake prototype made by diamond machining (right)

## Hardness and fracture toughness

Vickers hardness ( $H_V$ ) and toughness ( $K_{Ic}$ ) have been evaluated at room temperature on  $1/4 \mu\text{m}$  polished surfaces of all materials. At least five tests for each composite were carried out by Vickers indentation using a Testwell hardness tester. The hardness is determined by the ratio  $P/A$  where  $P$  is the force applied to the diamond and  $A$  is the surface area of the resulting indentation (in our case,  $P = 10 \text{ kgf} \sim 98 \text{ N}$ ). The fracture toughness ( $K_{Ic}$ ) is estimated by crack length measurement of the radial crack pattern formed around Vickers indents [24].

$$H_V = \frac{P}{A} = 0.001854 \times \frac{P}{d^2} \quad (1)$$

$$K_{Ic} = 0.0154 \times 10^{-6} \times \left( \frac{E}{H_V} \right)^{1/2} \times \frac{P}{c^{3/2}} \quad (2)$$

with  $H_V$  the hardness (GPa),  $P$  the load (N),  $a = d/2$  with  $d$  the average diagonal indentation mark length (mm),  $K_{Ic}$  the toughness ( $\text{MPa}\cdot\text{m}^{1/2}$ ),  $E$  the Young's modulus (GPa) and  $c$  the crack length from the centre of the indent to the crack tip (mm).

Very high levels of hardness and limited levels of toughness have been measured on the three selected compositions (table 5). In fact, all the materials exhibit hardness values close to that of tungsten carbide ( $H_V \sim 19.6 \text{ GPa}$ ) and toughness similar to that of common silicon nitride ( $K_{Ic} \sim 3.5 - 6 \text{ MPa}\cdot\text{m}^{1/2}$ ). SEM observations of the cracks have revealed that both intergranular and transgranular modes of propagation were present. Comparable behaviors are reported in the literature for this type of ceramic [20][21].

Composition	$H_{V10} / \text{GPa}$	$K_{Ic} / \text{MPa}\cdot\text{m}^{1/2}$	$E / \text{GPa}$
ZrB <sub>2</sub> /SiC	20.9 ± 1.9	4.3 ± 0.2	465 ± 15
ZrB <sub>2</sub> /SiC/TaSi <sub>2</sub>	18.1 ± 0.4	4.4 ± 0.3	446 ± 9
HfB <sub>2</sub> /SiC/TaSi <sub>2</sub>	18.1 ± 0.6	4.6 ± 0.2	498 ± 6

Table 5 – Hardness, toughness and Young's modulus of the three sintered materials

In comparison with metallic materials, the hardness of our compounds is considerably greater. For a nickel alloy such as Haynes 242, the  $H_V$  is around 2.7 GPa for instance. Moreover, the fracture toughness is also significantly lower:  $K_{Ic} = 24 \text{ MPa}\cdot\text{m}^{1/2}$  for the aluminum alloy 7075 for example.

## High temperature flexural strength

The three point bending test provides values for the flexural stress ( $\sigma_f$ ), the modulus of elasticity in bending ( $E_f$ ) and the flexural strain ( $\varepsilon_f$ ) of the material. The results shown in table 6 were obtained at different temperatures (20, 1000 and 1150°C), under air at atmospheric pressure, with a test speed of 0.3 mm/min and a support span of

30 mm (average dimension of samples:  $\sim 35.40 \times 5.20 \times 1.75 \text{ mm}^3$ ). For each material (manufactured with the optimized cycle) and each temperature, three to four samples were broken.

Composition	Property	20°C	Test temperature 1000°C	1150°C
		ZrB <sub>2</sub> /SiC	$\sigma_f$ (MPa) $E_f$ (GPa) $\varepsilon_f$ (%)	451 ± 90 194 ± 6 0.23 ± 0.04
ZrB <sub>2</sub> /SiC/TaSi <sub>2</sub>	$\sigma_f$ (MPa) $E_f$ (GPa) $\varepsilon_f$ (%)	688 ± 79 211 ± 13 0.32 ± 0.02	801 ± 40 181 ± 14 0.45 ± 0.04	864 ± 96 133 ± 13 0.65 ± 0.02
HfB <sub>2</sub> /SiC/TaSi <sub>2</sub>	$\sigma_f$ (MPa) $E_f$ (GPa) $\varepsilon_f$ (%)	869 ± 170 245 ± 13 0.36 ± 0.09	882 ± 146 203 ± 24 0.43 ± 0.05	1055 ± 189 178 ± 22 0.56 ± 0.13

Table 6 – Three point flexural strength (average value ± standard deviation)

Except for the reference material, for which some improvements in the manufacturing process are clearly necessary to recover the levels of the literature [21], the measured values are very satisfactory. Indeed, we can observe that for material comprising TaSi<sub>2</sub>, increasing temperature leads to higher flexural stresses, a strong increase of flexural strains and a moderate decrease in the flexion modulus. It is important to point out that, with these high levels of flexural stress (values over 1200 MPa have even been measured on HfB<sub>2</sub>/SiC/TaSi<sub>2</sub> samples at 1150°C), it is possible to envisage the manufacturing of future high-strength sharp UHTC components.

## Thermal and optical properties

### Coefficient of thermal expansion

The thermal expansion behavior of the three hot pressed materials has been characterized between room temperature and 1300°C by using an Adamel Lhomargy DI.24 dilatometer (under argon flow). The coefficient of thermal expansion ( $\alpha$  tangent in °C<sup>-1</sup>) is calculated from the following formula:

$$\alpha(T) = \frac{1}{l(T)} \times \frac{dl(T)}{dT} \quad (3)$$

The reference temperature is room temperature (25°C). The recorded values are presented in figure 3. The correlations for the CTE of each composition are given by the following expressions with  $T$  in °C units:

$$\text{for ZrB}_2/\text{SiC} \quad \alpha(T) = 4.654676 \cdot 10^{-10} T + 6.844813 \cdot 10^{-6} \quad (4)$$

$$\text{for ZrB}_2/\text{SiC}/\text{TaSi}_2 \quad \alpha(T) = 4.002628 \cdot 10^{-10} T + 7.157354 \cdot 10^{-6} \quad (5)$$

$$\text{for HfB}_2/\text{SiC}/\text{TaSi}_2 \quad \alpha(T) = 1.225332 \cdot 10^{-10} T + 7.216565 \cdot 10^{-6} \quad (6)$$

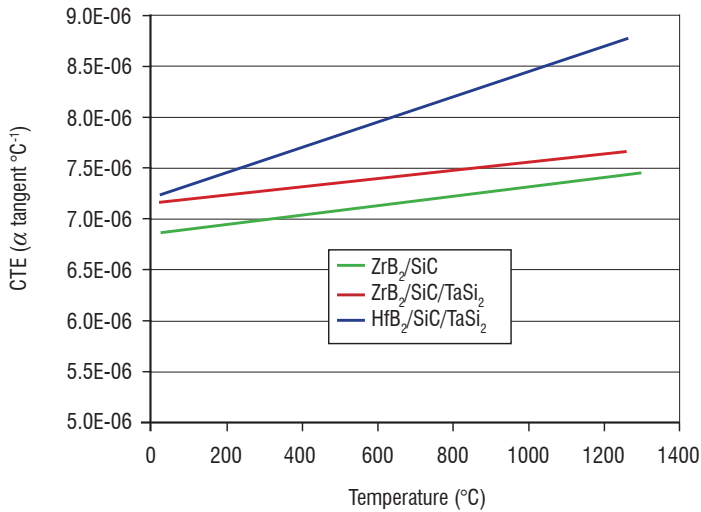


Figure 3 – Coefficients of thermal expansion of the three selected materials

Thus between 25 and 1250°C, the average values of CTE are:

- $ZrB_2/SiC \sim 7.1 \cdot 10^{-6} \text{ } ^\circ C^{-1}$
- $ZrB_2/SiC/TaSi_2 \sim 7.4 \cdot 10^{-6} \text{ } ^\circ C^{-1}$
- $HfB_2/SiC/TaSi_2 \sim 8.0 \cdot 10^{-6} \text{ } ^\circ C^{-1}$

These values are in good agreement with the data available in the literature on similar materials [22][25]. In comparison to advanced CMC (SiC/SiC or C/SiC), these coefficients are quite high and closer to some ceramics like alumina ( $\alpha_{0-1000^\circ C} = 8 \cdot 10^{-6} \text{ } ^\circ C^{-1}$ ). However, they are twice as low as for metallic materials such as nickel alloys ( $\alpha_{25-1000^\circ C} = 16.3 \cdot 10^{-6} \text{ } ^\circ C^{-1}$  for Inconel 617 for instance).

#### Thermal conductivity

The thermal conductivity ( $\lambda$ ) was calculated from the correlation functions of thermal diffusivity ( $D$ ), specific heat capacity ( $C_p$ ) and density ( $\rho$ ) according to the formula:

$$\lambda(T) = D(T) \times \rho(T) \times C_p(T) \quad (7)$$

The correlations for density were deduced from the CTE measurements. As for diffusivity and specific heat capacity, they were determined by a laser flash technique [26] from room temperature to 1200°C (under argon) on 20 mm diameter and 2 mm thick discs. These characterizations were carried out on the first generation of materials (sintered before the improvements relating to powder blends attrition) and only on monoliths with TaSi<sub>2</sub>. The calculated values are presented in figure 4 and the correlations for  $\lambda$  are given by the following expressions (in these formulas, T is in °C units):

- for  $ZrB_2/SiC/TaSi_2$

$$\lambda(T) = 2.6693 \cdot 10^{-8} T^3 - 6.0102 \cdot 10^{-5} T^2 + 3.0995 \cdot 10^{-2} T + 3.6168 \cdot 10^{+1} \quad (8)$$

- for  $HfB_2/SiC/TaSi_2$

$$\lambda(T) = 1.7971 \cdot 10^{-8} T^3 - 3.8412 \cdot 10^{-5} T^2 + 1.6151 \cdot 10^{-2} T + 3.2240 \cdot 10^{+1} \quad (9)$$

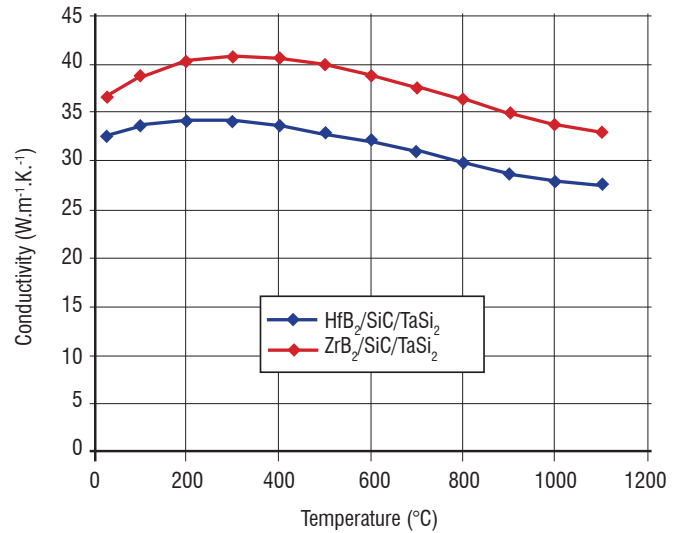


Figure 4 – Thermal conductivity

From 20 to 1200°C, the thermal conductivities of the characterized materials (sintered from non-optimized mixtures) are higher than 25 W.m<sup>-1</sup>.K<sup>-1</sup>. In fact, the thermal conductivities of diboride-based UHTC are typically high [27][28], in comparison with those of many other ceramics (table 7) and are a result of both a lattice (vibrations) and an electronic contribution to phonon transport [30]. These values are also higher than for some alloys and CMC (for example: at 300K,  $\lambda = 13.6 \text{ W.m}^{-1}.\text{K}^{-1}$  for Inconel 617 and  $\lambda \sim 14.5 \text{ W.m}^{-1}.\text{K}^{-1}$  for a standard C/C-SiC). This ability to easily transport heat is one of the most important advantages of these materials. Indeed, their high conductivity allows heat to be conducted from a high heating area to a region of lower heating, where it is then re-radiated into the atmosphere. Furthermore, their high level of conduction gives them good thermal shock resistance.

Material	$\lambda / \text{W/m K}$
Si <sub>3</sub> N <sub>4</sub> (Kyocera SN-220)	15.5 (293K) - 13 (1273K)
Al <sub>2</sub> O <sub>3</sub> (Kyocera A-479)	24 (293K) - 5 (1273K)
ZrO <sub>2</sub> (Kyocera Z-701N)	4 (293K) - 3 (1273K)

Table 7 – Thermal conductivity of some different ceramics [29]

#### Total hemispherical emissivity

As for thermal conductivity, total hemispherical emissivity ( $\epsilon$ ) determinations have been carried out on the first generation of materials and only on monoliths comprising TaSi<sub>2</sub> (total hemispherical emissivity values are deduced from spectral thermal emissivity measurements [31]). The assessment of each material was done on two parallelepiped samples (16 x 8 x 2 mm<sup>3</sup>), from 200 to 800°C, under argon, before and after an oxidation treatment at 1000°C.

Emissivity values for oxidized materials are presented in figure 5 and the correlations for  $\varepsilon$  are given by the following expressions (in these formulas,  $T$  is in °C units):

- for  $ZrB_2/SiC/TaSi_2$

$$\varepsilon(T) = -2.9689 \cdot 10^{-10} T^3 + 2.4882 \cdot 10^{-7} T^2 + 2.3138 \cdot 10^{-4} T + 7.6225 \cdot 10^{-1} \quad (10)$$

- for  $HfB_2/SiC/TaSi_2$

$$\varepsilon(T) = -7.5962 \cdot 10^{-10} T^3 + 1.0203 \cdot 10^{-6} T^2 - 2.2331 \cdot 10^{-4} T + 8.3449 \cdot 10^{-1} \quad (11)$$

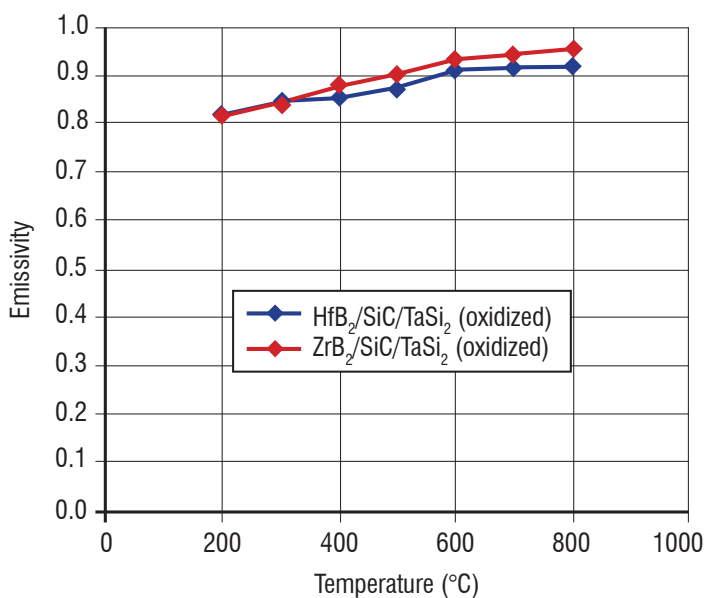


Figure 5 – Total hemispherical emissivity (after oxidation)

In the temperature range studied, oxidized surfaces lead to emissivities higher than 0.8. This level of emissivity is entirely sufficient for the components for which UHTC monoliths are developed (leading edges and air intakes). In these applications, a high emissivity is indeed desirable, as it would reradiate much of the energy from the surface, eliminating some of the energy that the piece would otherwise have to handle. We can add that similar values are generally observed on classical CMC such as C/SiC or SiC/SiC.

### Oxidation and thermal shock resistance

#### Furnace oxidation under stagnant air

The thermal shock behavior and the long resistance time under oxidative atmosphere and at high temperature have been assessed by thermal treatments of several samples at 1000°C under stagnant air at atmospheric pressure. Cumulative times in furnaces of up to 1000 hours were administered on the three selected compositions. The oxidation kinetics were obtained by following material weight variations versus time and the thermal shock resistance was assessed simply by several sudden insertions and extractions of the samples.

For each material, more than 12 cycles of insertion/extraction (*i.e.* at least 24 thermal shocks) were achieved without any problems. In fact, the materials fully maintained their integrity. No cracks

appeared and no destructive oxidation was observed. Thus, under the previous test parameters, all the compositions exhibited good thermal shock resistance. This is due to a large extent to the high thermal conductivity of these materials.

The specific weight changes vs. oxidation time are shown in figure 6. Oxidation kinetics slow down with time and with the samples tested the total weight variations are very limited (< 0.3 % after 1000 h). In addition, as observed by SEM, there is formation of a protective layer on the surface. This protective layer is divided in two parts: a SiO<sub>2</sub> rich glass as the outermost coat (~7 μm thick) and an intermediate layer in the process of being oxidized (~20 μm thick). Very similar behavior has been also observed in samples tested in an arc-jet facility (figure 7).

These results allow us to conclude that the selected materials exhibit good oxidation resistance with the test parameters and conditions of this study.

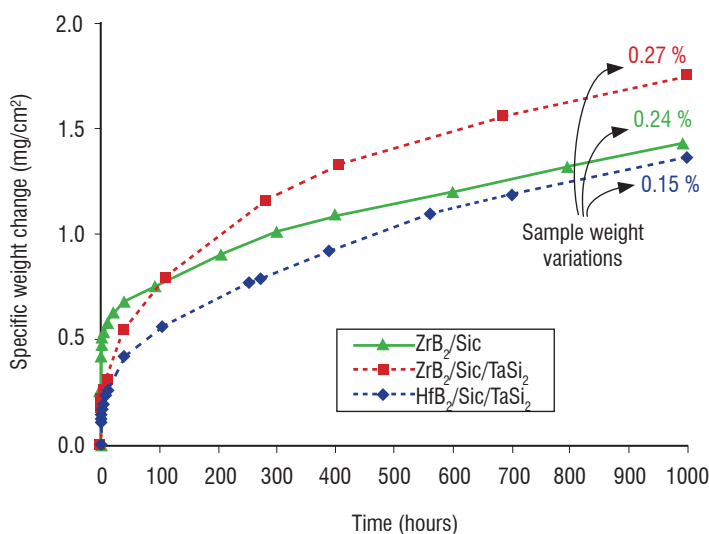


Figure 6 – Oxidation kinetics of the three selected materials

#### Arc-jet tests

In order to investigate the thermal and chemical resistance of the three selected materials in more realistic conditions (close to hypersonic flight), a test campaign was carried out under high-enthalpy hypersonic flow in an arc-jet facility at DLR Cologne (L2K) [32]. First, four disc-shaped samples ( $\varnothing$  26.5 mm,  $e$  = 4 mm) of each composition were machined. Then, with these specific samples, several tests were carried out from 1100 to 1500°C. The test at 1100°C was defined as the baseline test condition with regard to the ATLLAS objectives (hypersonic flights at Mach 6 in Earth atmosphere). Afterwards, higher enthalpy and temperature levels were applied with three other test conditions in order to check the materials' capabilities:

sample A	2 cycles	test of 300 s at 1100°C + test of 600 s at 1100°C
sample B	2 cycles	test of 300 s at 1100°C + test of 600 s at 1300°C
sample C	1 cycle	test of 600 s at 1400°C
sample D	1 cycle	test of 600 s at 1500°C

The samples' resistance to high enthalpy flow was assessed by several measurements (weighing, thickness checking), and by photographs

before and after each test and finally SEM observations of a few samples on both oxidized surfaces and polished cross-sections of discs (figure 7). In addition, videos and photographs were recorded during all of the experiments (see for example figure 8 and video).

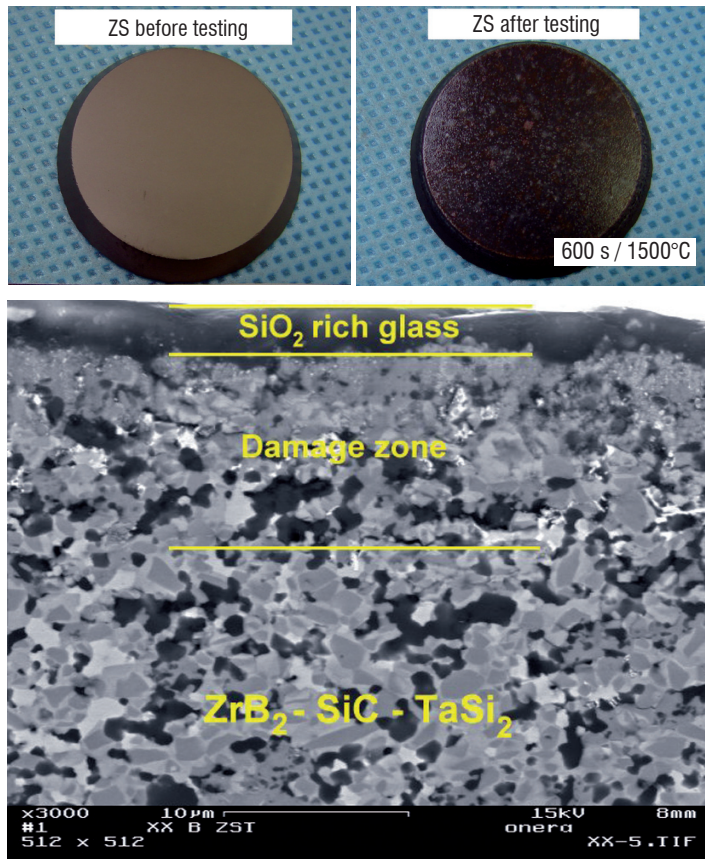


Figure 7 –  $ZrB_2/SiC$  disc before and after a test at  $1500^\circ C$  (top) and cross-sectioned.  $ZrB_2/SiC/TaSi_2$  disc after 2 successive cycles at  $1100$  and  $1300^\circ C$  (bottom)

The results of this test campaign were very satisfactory. For each condition, good material resistance was detected (the most important mass and thickness variations observed during this campaign were quite limited:  $\Delta M_{max} = 0.33\%$  and  $\Delta e = 50 \mu m$ ). As previously observed by SEM on oxidized materials (tests under stagnant air), there is again formation of a thin glass layer on the surface and

underneath an intermediate layer in the process of being oxidized (SiC-depleted layer) [33]. Thermodynamically,  $ZrB_2$ ,  $HfB_2$  and SiC should oxidize when exposed to air. However, below  $1200^\circ C$ , it is reported in the literature that the oxidation of  $ZrB_2$  (or  $HfB_2$ ) is more rapid than that of SiC. Then there is production of a continuous protective oxide layer of  $B_2O_3$  (l) with entrained  $ZrO_2$  (or  $HfO_2$ ) which prevents  $ZrB_2$  (or  $HfB_2$ ) from being further oxidized. At higher temperatures,  $B_2O_3$  (l) evaporates due to its high vapor pressure and consequently the rate of SiC oxidation increases, inducing the formation of a  $SiO_2$  rich glass on the surface [6]. Up to  $1600^\circ C$ ,  $TaSi_2$  addition improves oxidation resistance because it reduces oxygen vacancy concentration in  $ZrO_2$ . However, it is important to note that Opila et al. has shown that Ta additions are less effective in  $HfB_2$  based materials [15].

In conclusion, under ATLLAS conditions, cumulative durations up to 900 s are performed without any problems (for all the selected compositions). Very good sample-to-sample reproducibility and a lack of sensitivity to thermal load cycling have been demonstrated. In addition, all the selected materials are able to sustain higher thermal loads (up to  $1500^\circ C/600$  s). Thus, the requirements for the sharp leading edges and air intakes of the ATLLAS vehicle are well fulfilled. This good thermal-oxidative stability in severe environments is certainly one of the most important results of this work on UHTC materials. It is also interesting to note that several studies have demonstrated the excellent behavior of typical UHTC leading edges under arc-jet testing compared with more traditional composites like C/SiC for instance [34]. However, for long-term use under hypersonic conditions ( $\sim 25,000$  cycles), some confirmations of the high resistance of our materials will be necessary to completely validate the solutions.

#### Possible design of a UHTC sharp leading edge

Due to the high level of properties demonstrated previously, it seems possible to envisage the future making of sharp components based on the best selected UHTC materials. With better knowledge of these specific materials, it should now be easier to design some examples of what could be a leading edge or an air intake of the ATLLAS vehicle. As a matter of fact, the best way to use monolithic UHTC materials for manufacturing sharp components seems to be to combine these materials with others (CMC notably). Thus, the UHTC part would be placed as an insert in front of the structural component in order to use only UHTC pieces of limited size (figure 9). This allows for optimization

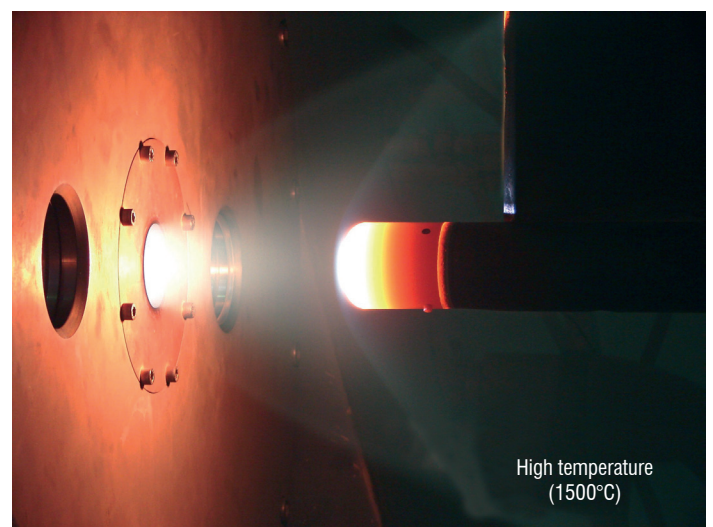
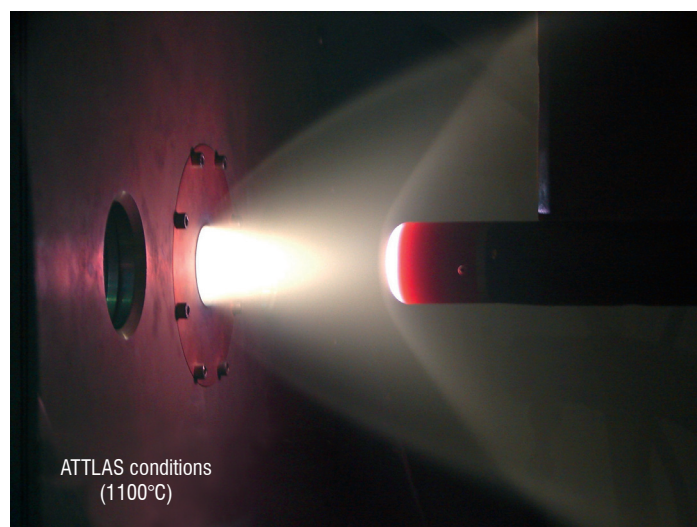


Figure 8 – Flow field around sample holder at different test conditions (shapes of the bow shock and the free stream boundary)  
<http://www.aerospacelab-journal.org/al3/Ultra-High-Temperature-Ceramics>

of the element involved (performance, weight and cost in particular). However, it is important to note that the attachment design needs to be properly addressed to minimize thermal stresses. For example, it would be possible to avoid the contact of the UHTC element with cooler sub-components in the structure in order to reduce bearing stresses at the attachment location [35]. Moreover, in order to avoid possible crack propagation in the UHTC component and also to make the manufacturing easier, the design calls for the leading edge to be comprised of multiple UHTC tiles or segments rather than a one-piece continuous edge [36].

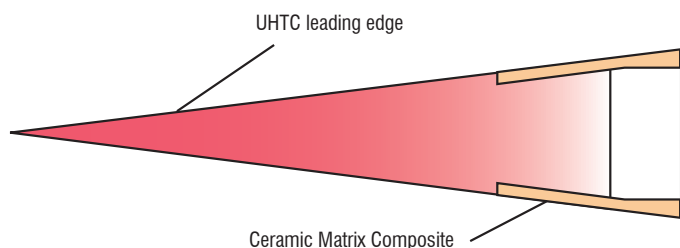


Figure 9 – Possible schematic design of a UHTC sharp component

### Outlook: materials for propulsion use

Another major challenge for the future is the development of new materials able to meet the strict requirements of the next generation of propulsion systems for civilian and military uses. These include

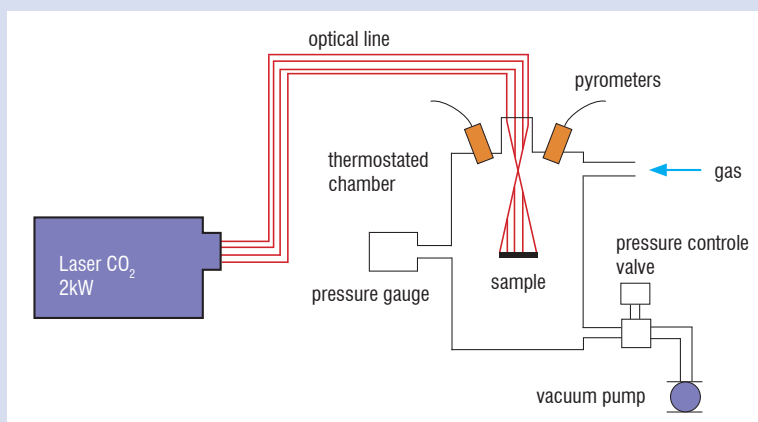
for example specific engine components for hypersonic vehicles (thin uncooled injectors for hydrogen) or elements for high-energy propellant propulsion (hot gas vanes). For this type of application, and for the most rigorous hypersonic uses, there are needs for materials that can withstand 2000 to 3000°C. Onera is therefore involved in several programs (ATLLAS 2 for instance) to assess UHTC materials that could meet these new requirements (with monoliths and composite coatings). Further information regarding ATLLAS 2 can be found on [www.esa.int/techresources/atllas\\_II](http://www.esa.int/techresources/atllas_II). In propulsion applications, at temperatures exceeding 2000°C, one of the main problems is the resistance to oxidation and corrosion of the materials which are in contact with combustion gases. These gases contain highly oxidative and corrosive chemical species (water vapor, CO<sub>2</sub>, CO and HCl for instance), and we know that low oxidation rate materials, which form pure scales of SiO<sub>2</sub>, Al<sub>2</sub>O<sub>3</sub>, Cr<sub>2</sub>O<sub>3</sub>, or BeO cannot be used at temperatures above 1800°C due to the disruption of high vapor pressures which arise at the interphase of the base material and the scale [37]. Therefore, diboride/SiC materials with specific additives (rare earth oxides or LaB<sub>6</sub> for example) to improve their resistance to oxidation above 2000°C [38] and new compounds based on oxide blends or carbide/nitride mixtures are currently being studied in our laboratories. In order to evaluate the level of resistance to oxidation of these new materials with relative ease, a custom-designed facility is used: the BLOX 4, which is a 4th generation Laser Oxidation Analysis facility (see box 2). This system simulates the effects of various atmospheres (water vapor for example) on the behavior of UHTC materials at high temperatures.

### Box 2 - Laser Oxidation Analysis Facility (BLOX)



Figure B2-01 – BLOX facility at Palaiseau center

The 4<sup>th</sup> laser oxidation analysis facility (BLOX) is a custom-made device used for thermal characterization of materials at very high temperatures in controlled atmospheres (air, N<sub>2</sub>, O<sub>2</sub>, Ar, CO<sub>2</sub>, water vapor, H<sub>2</sub>...) at pressures ranging from a few millibars to 4 bars. The use of a high power CO<sub>2</sub> laser (2kW) can generate temperatures of 2000°C or higher. The sample temperature is measured with pyrometers as seen in the general diagram of BLOX.



Materials can be characterized under intense, continuous or impulse heat flux and the very low thermal inertia allows temperature cycling at high frequencies and very rapid temperature rises.

In addition, due to the selected constituents of the previous UHTC compounds, very high temperatures and pressures would be required to sinter the powders. For this reason, a promising method called Spark Plasma Sintering (SPS) or Field Assisted Sintering Technology (FAST) has been selected to manufacture UHTC monoliths. Using this modified hot pressing process in which electric current runs through the pressing mold and the component, very rapid heating times and short sintering cycles can be achieved [39]. In addition, its operation is easy and it enables ceramics to become fully dense at comparatively low temperatures and with limited grain growth (very fine microstructures are thus possible).

## Conclusion

Hypersonic, atmosphere re-entry and rocket propulsion applications provide some unique thermal-structural challenges (sharp leading edges, air intakes, vanes, etc.). In order to fulfill the requirements of these components, some specific materials are compulsory (UHTC). Indeed, thanks to their unique combination of mechanical, thermal and chemical properties, UHTCs are a promising technology for use in a number of high temperature structural applications.

ZrB<sub>2</sub>-SiC, ZrB<sub>2</sub>-SiC-TaSi<sub>2</sub> and HfB<sub>2</sub>-SiC-TaSi<sub>2</sub> were studied for leading edge applications in the ATLLAS project. These compositions were sintered by hot pressing between 1700 and 1800°C and reached 98% of the theoretical density. They possess attractive properties: high hardness, high flexural stress, good machinability, high emissivity. Another attractive feature of these materials is their relatively high thermal conductivity which gives them better thermal shock resistance than most insulating materials and allows heat to be conducted from the leading edge to a region of lower heating, where it is re-radiated into the atmosphere. In addition, these materials exhibit good resistance to oxidation at very high temperatures (>1500°C) due to the formation of a glassy protective layer. Oxygen diffusion is slowed down through this oxide layer and ZrB<sub>2</sub> is then prevented from undergoing further oxidation. All these properties allow these materials to fulfill the requirements to sustain hypersonic flight conditions as demonstrated in the ATLLAS project.

These kinds of materials are also of great value for higher temperature applications (i.e. 2000°C and more). New characterization devices are needed to test them in environments as close to real conditions as possible. A custom-made device is being used in Onera laboratories to reach 2000°C and higher in oxidizing atmospheres ■

## Acknowledgements

This work was carried out within the "Aerodynamic and Thermal Load Interactions with Lightweight Advanced Materials for High Speed Flight" project investigating high-speed transport. ATLLAS, coordinated by ESA-ESTEC, is supported by the EU within the 6th Framework Programme Priority 1.4, Aeronautic and Space, Contract n° AST5-CT-2006-030729.

We would like to thank B. Esser and A. Gülhan for the test campaign carried out in the L2K arc jet facility of DLR Cologne [32].

## References

- [1] E. CLOUGHERTY, D. KALISH and E. PETERS - *Research and Development of Refractory Oxidation Resistant Diborides*. Technical Report AFML-TR-68-190, 1968.
- [2] G. V. SAMSONOV - *Refractory Transition Metal Compounds: High Temperature Cermets*. Academic Press, New York, 1964.
- [3] M.M. OPEKA, I.G. TALMY and J.A. ZAYKOSKI - *Oxidation-Based Materials Selection for 2000°C + Hypersonic Aerosurfaces: Theoretical Considerations and Historical Experience*. Journal of Materials Science 39, 5887-5904, 2004.
- [4] S.R. LEVINE, E.J. OPILA, M.C. HALBIG, J.D. KISER, M. SINGH and J.A. SALEM - *Evaluation of Ultra-High Temperature Ceramics for Aero propulsion Use*. J. European Ceramic Society 22, 2757-2767, 2002.
- [5] J. HAN, P. HU, X. ZHANG and S. MENG - *Oxidation Behavior of Zirconium Diboride-Silicon Carbide at 1800 °C*. Scripta Materialia 57, 825-828, 2007.
- [6] W.G. FAHRENHOLTZ - *Thermodynamic Analysis of ZrB<sub>2</sub>-SiC Oxidation: Formation of a SiC-Depleted Region*. J. American Ceramic Society 90, 43-148, 2007.
- [7] F. MONTEVERDE and A. BELLOSI - *Oxidation of ZrB<sub>2</sub>-Based Ceramics in Dry Air*. J. Electrochemical Society 150 [11], B552-B559, 2003.
- [8] D.A. KONTINOS, K. GEE and D.K. PRABHU - *Temperature Constraints at the Sharp Leading Edge of a Crew Transfer Vehicle*. American Inst. of Aeronautics & Astronautics, 2001-2886, 2001.
- [9] W.G. FAHRENHOLTZ, G.E. HILMAS, I. G. TALMY and J. A. ZAYKOSKI - *Refractory Diborides of Zirconium and Hafnium*. J. American Ceramic Society 90, 1347-1364, 2007.
- [10] J. STEELANT - *Atlas: Aero-Thermal Loaded Material Investigations for High-Speed Vehicles*. 15<sup>th</sup> AIAA International Space Planes and Hypersonic Systems and Technologies Conference, Dayton, Ohio, 2008.
- [11] J.F. JUSTIN - *Investigations of High Temperature Ceramics for Sharp Leading Edges or Air Intakes of Hypersonic Vehicles*. 3<sup>rd</sup> European Conference for AeroSpace Sciences, Versailles, France, CD-ROM ISBN 978-2-930389-47-8, 2009.
- [12] A. EZIS and J.A. RUBIN - *Hot Pressing*. Engineered Materials Handbook, vol 4, Ceramics and Glasses, 186-193, 1991.
- [13] G.E. GAZZA - *Pressure Densification*. Engineered Materials Handbook, vol 4, Ceramic and Glasses, 296-303, 1991.
- [14] W.C. TRIP, H.H. DAVIS and H.C. GRAHAM - *Effect of a SiC Addition on the Oxidation of ZrB<sub>2</sub>*. American Ceramic Society Bulletin, vol 52 [8], 612-616, 1973.
- [15] E. OPILA and S. LEVINE - *Oxidation of ZrB<sub>2</sub>- And HfB<sub>2</sub>-Based Ultra-High Temperature Ceramics: Effect of Ta Additions*. Journal of Materials Science 39, 5969-5977, 2004.
- [16] T.H. SQUIRE and J. MARSCHALL - *Material Property Requirements for Analysis and Design of UHTC Components in Hypersonic Applications*. J. European Ceramic Society 30, 2239-2251, 2010.
- [17] R. RIEDEL - *Handbook of Ceramic Hard Materials*. WILEY-VCH, 2000.
- [18] N. FAULK - *Electrical Discharge Machining*. Engineered Materials Handbook, vol 4, Ceramics and Glasses, 371-376, 1991.
- [19] ASTM Standard E1876-09 - *Standard Test Method for Dynamic Young's Modulus, Shear Modulus, and Poisson's Ratio by Impulse Excitation of Vibration*.

- [20] S.Q. GUO and al - *Mechanical Properties of Hot-Pressed ZrB<sub>2</sub>-MoSi<sub>2</sub>-SiC Composites*. J. European Ceramic Society 28, 1891-1898, 2008.
- [21] A.L. CHAMBERLAIN, W.G. FAHRENHOLTZ and G.E. HILMAS - *High-Strength Zirconium Diboride-Based Ceramics*. J. American Ceramic Society 87, 1170-1172, 2004.
- [22] F. MONTEVERDE - *Ultra-High Temperature HfB<sub>2</sub>-SiC Ceramics Consolidated by Hot-Pressing and Spark Plasma Sintering*. Journal of Alloys and Compounds 428, 197-205, 2007.
- [23] F. MONTEVERDE, A. BELLOSI and L. SCATTEIA - *Processing and Properties of Ultra-High Temperature Ceramics for Space Applications*. Materials Science and Engineering: A. 485, 415-421, 2008.
- [24] G.R. ANSTIS, P. CHANTIKUL, B.R. LAWN and D.B. MARSHALL - *A Critical Evaluation of Indentation Techniques for Measuring Fracture Toughness: I. Direct Crack Measurements*. J. American Ceramic Society 64, 534-553, 1981.
- [25] A. FRANCESE - *Numerical and Experimental Study of UHTC Materials for Atmospheric Re-Entry*. Dottorato di ricerca in ingegneria aerospaziale, 2007.
- [26] W.J. PARKER, R.J. JENKINS, C.P. BUTLER and G.L. ABBOT - *Flash Method of Determining Thermal Diffusivity, Heat Capacity, and Thermal Conductivity*. J. Applied Physics 32, 1679-1684, 1961.
- [27] R. LOEHMAN, E. CORRAL, H.P. DUMM and al - *Ultra-High Temperature Ceramics for Hypersonic Vehicle Applications*. Sandia Report, SAND 2006-2925, 2006.
- [28] M. GASCH, S. JOHNSON and J. MARSCHALL - *Thermal Conductivity Characterization of Hafnium Diboride-Based Ultra-High-Temperature Ceramics*. J. American Ceramic Society 91, 1423-1432, 2008.
- [29] *Characteristics of Kyocera Technical Ceramics*. [http://americas.kyocera.com/kicc/pdf/Kyocera\\_Material\\_Characteristics.pdf](http://americas.kyocera.com/kicc/pdf/Kyocera_Material_Characteristics.pdf).
- [30] R. A. CUTLER - *Engineering Properties of Borides*. Engineered Materials Handbook, vol 4, Ceramics and Glasses, 787-803, 1991.
- [31] D. DEMANGE and M. BEJET - *New Methods for Measuring the Thermal Emissivity of Semi-Transparent and Opaque Materials*. 8<sup>th</sup> International Conference on Quantitative Infrared Thermography, Padova, 2006.
- [32] B. ESSER - *Thermal Characterisation of Onera's Uhtc Materials*. Deliverable D.3.2.6 of ATLLAS project, 2009.
- [33] T. PARTHASARATHY, R. RAPP, M. OPEKA and R. KERANS - *A Model for the Oxidation of ZrB<sub>2</sub>, HfB<sub>2</sub> and TiB<sub>2</sub>*. Acta Materialia 55, 5999-6010, 2007.
- [34] X. ZHANG and al - *Ablation Behavior Of ZrB<sub>2</sub>-SiC Ultra High Temperature Ceramics under Simulated Atmospheric Re-Entry Conditions*. Composites Science and Technology 68, 1718-1726, 2008.
- [35] D.J. THOMAS - *Design and Analysis of Uhtc Leading Edge Attachment*. NASA/CR-2002-211505, Glenn research Center, 2002.
- [36] T. KOWALSKI, K. BUESKING, P. KOLODZIEJ and J. BULL - *A Thermostructural Analysis of a Diboride Composite Leading Edge*. NASA Technical Memorandum 110407, 1996.
- [37] K. UPAHYA, J.-M YANG and W. P. HOFFMAN - *Materials for Ultrahigh Temperature Structural Applications*. The American Ceramic Society Bulletin, 51-56, 1997.
- [38] J. HAN, P. HU, X. ZHANG, S. MENG and W. HAN - *Oxidation-Resistant ZrB<sub>2</sub>-SiC Composites at 2200 °C*. Composites Science and Technology 68, 799-806, 2008.
- [39] H.U. KESSEL, J. HENNICKE, J. SCHMIDT, T. WEIßGÄRBER, B. F. KIEBACK, M. HERRMANN and J. RÄTHEL - *"Fast" Field Assisted Sintering Technology - A New Process for the Production of Metallic and Ceramic Sintering Materials*.

## Acronyms

UHTC (Ultra High Temperature Ceramic)	CMC (Ceramic Matrix Composite)
ATLLAS (Aerodynamic and Thermal Load Interactions with Lightweight Advanced Materials for High Speed Flight)	C/C (Carbon / Carbon Composite)
ESA-ESTEC (European Space Research and Technology Centre of the European Space Agency)	C/SiC (Carbon / Silicon Carbide Composite)
DLR (Deutsches Zentrum für Luft und Raumfahrt)	SiC/SiC (Silicon Carbide / Silicon Carbide Composite)
SST (Supersonic Transport)	EDM (Electrical Discharge Machining)
LE (Leading Edge)	SEM (Scanning Electron Microscopy)
YTZ (Yttrium stabilized Zirconia)	CTE (Coefficient of Thermal Expansion)
HP (Hot Pressing)	SPS (Spark Plasma Sintering)
	FAST (Field Assisted Sintering Technique)
	BLOX (Laser OXidation analysis facility)

## AUTHORS



**Jean-François Justin** is a research engineer working within the Thermostructural and Functional Composites unit (CTF) of the Composite Materials and Structures Department (DMSC). He graduated from the "Conservatoire National des Arts et Métiers". Since he joined Onera in 1989, he has been concerned with the development of monolithic ceramics and Ceramic Matrix Composites for functional applications (combustion chambers, stealth materials, engine blades, leading edges, air intakes ...). He has been also involved in the improvement of CMC processing routes and CVD coatings. Currently, his research field is mainly focused on Ultra-High Temperature Ceramics (notably within the framework of the European project ATLLAS II).



**Aurélie Jankowiak** After graduating from ENSCI in 2005, she received a PhD in Materials Science from the University of Limoges (2008). She has been working since 2009 in the Composite Materials and Structures Department of Onera. Her research field is mainly focused on high temperature materials for functional applications (combustion chambers, engine blades, leading edge).